Improved Zero-Current Transition Converters For High Power Applications*

Hengchun Mao, Fred C. Lee, Xunwei Zhou, and Dushan Boroyevich

Virginia Power Electronics Center
The Bradley Department of Electrical Engineering
Virginia Polytechnic Institute and State University
Blacksburg, VA 24061-0111
Fax: (540) 231-6390, Email: hmao@vtvm1.cc.vt.edu

Abstract - Existing Zero-Current Transition (ZCT) converters do not solve main switch turn-on problems and require auxiliary switches to be turned off with high current, and therefore are not suitable for high power applications. Novel ZCT schemes proposed in this paper enable all main switches and auxiliary switches to be turned on and off under zero current conditions. The zero-current switching at both turn-on and turn-off not only reduces switching losses significantly, but also eliminates the necessity of passive snubbers due to the much reduced switch stress. The cost of the auxiliary switches can be reduced compared to the existing ZCT schemes due to their zero-current turn-off. The proposed technology is well suited for dc-dc and three-phase converters with IGBTs, MCTs and GTOs. Theoretical analysis, computer simulation and experimental results are presented to explain the proposed schemes.

I. INTRODUCTION

Power semiconductor switches in high power applications are subject to high switching stresses and switching losses. In conventional designs, significant derating of device voltage and current ratings and elaborate passive snubbers have to be used due to the switching stresses, and the switching frequency is limited to low frequency ranges. In recent years, various soft-switching techniques have been proposed to alleviate these problems. Significant performance improvements as well as cost, size and weight reduction can be achieved with the help of soft switching. A successful soft switching scheme for high power applications should reduce the switching losses, diode reverse recovery, and switching stress for all main and auxiliary switches without increasing the device voltage rating, because the device voltage margin is usually small and the thermal management very difficult. The recently developed zero-voltage transition (ZVT) [7] and zero-current transition (ZCT) [1] PWM techniques incorporate soft switching into PWM converters, so that the switching losses can be reduced with minimum voltage/current stresses and circulating energy. The ZVT technique forces the voltage of a switch to zero before its turn-on, to practically eliminate switch turn-on loss. The switch turn-off loss, which is usually the dominating switching loss in high power applications, cannot be alleviated effectively with ZVT technique, because a capacitor snubber sized for high frequency operation has only marginal effect on the turn-off loss. The ZCT technique can significantly reduce the switch turn-off loss by forcing the switch current to zero prior to its turn-off. A ZCT boost converter proposed in [1] is shown in Fig. 1(a), where the auxiliary circuit is shown within the dotted frame. The key waveforms of the circuit operation are shown in Fig. 1(b). As can be seen from Fig. 1(b), the current of the main switch is reduced to zero prior to its turn-off. However, the turn-on of the main switch is not affected by the auxiliary circuit, and severe diode reverse recovery causes high turn-on loss in the switch. Moreover, the auxiliary switch turn-off current (at the moment t_3) is the same as the inductor current I, i.e. the same as the main switch turn-off current in the hard-switched converter. Therefore, this scheme can achieve efficiency improvement only if Sx has much lower turn-off loss than S (such as in the low power and low voltage applications where MOSFETs with low turn-off loss can be used to implement the auxiliary switch), and is not suitable for high power applications. Additionally, high current devices (>100 A) have limited turn-off capability, so the auxiliary switch would often be of similar size and cost as the main switch. The current commutation techniques for SCR converters [3, 4] are not suitable for gate controlled devices because they do not solve diode reverse recovery problem, have high power loss in the auxiliary circuit, and some of them increase switch voltage stress or require switches to block negative voltage.

In this paper, several new ZCT schemes are proposed and investigated to further improve the ZCT technique in [1]. With modified control and topology, all main switches and auxiliary switches are switched on and off under zero-current condition, so the switching losses and stresses are reduced significantly. The zero-current switching of the auxiliary

* This work is supported in part by Naval Surface Warfare Center through a contract from Westinghouse Electric Company.

0-7803-3544-9/96 $5.00 © 1996 IEEE

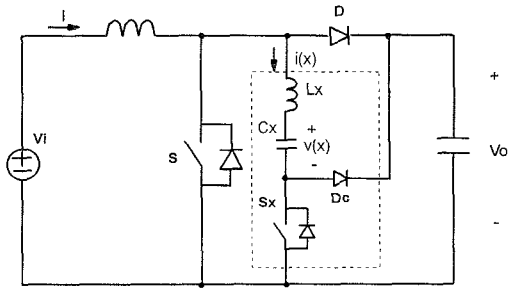

(a) Topology.

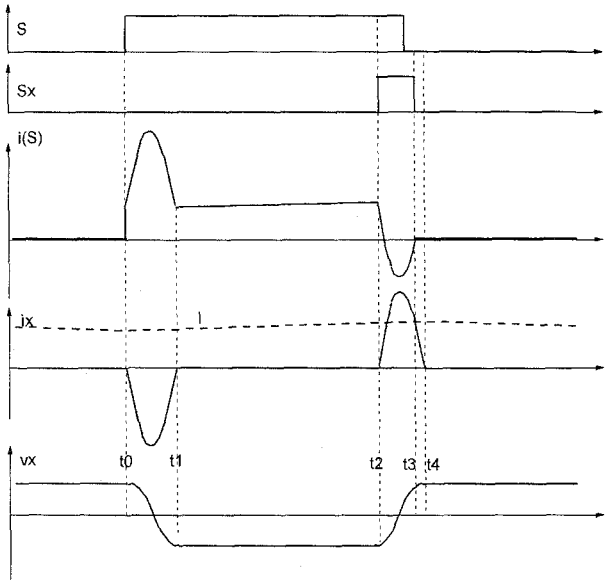

(b) Operational Waveforms Proposed in [1].

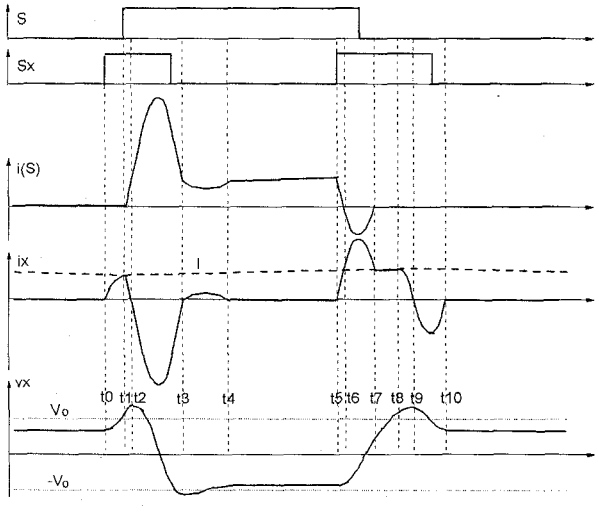

(c) Waveforms with Proposed Modified Control.

Fig. 1. ZCT PWM Boost Converter Proposed in [1]

switches also allows the use of low power rating device and low-conduction-loss devices, such as MCTs and IGBTs, in the auxiliary circuit. Since all PWM converters can be constructed using a well-known PWM cell, we will discuss the soft switching schemes with a boost converter as an example, and extend it to other converters through the concept of soft-switched PWM cell.

II. A NEW ZCT BOOST RECTIFIER

The drawbacks of the ZCT topology shown in Fig. 1(a) can be overcome to some degree with a modified control. By letting the auxiliary switch conduct longer, its current is reduced to zero due to the resonance between Lx and Cx, so the auxiliary switch can be turned off under zero-current condition. The main switch turn-on current can also be reduced by the ZCT circuit, if the auxiliary switch is turned on before the main switch turn-on. Fig. 1(c) shows the key waveforms with this modified control. As can been seen from Fig. 1(c), both the main switch and auxiliary switch are turned on and off with zero-current, so switching loss can be reduced significantly. However, the current peak in the auxiliary circuit is very high, and causes high conduction loss. The current peak can be reduced by modifying the auxiliary circuit. The proposed new ZCT scheme is shown in Fig. 2(a). The modified auxiliary circuit, shown within the dotted frame, consists of a resonant inductor Lx, a resonant capacitor Cx, an auxiliary switch Sx together with its parallel diode Dx, and a clamp diode Dc. This topology is similar to the one in Fig. 1(a), with only major difference in the arrangement of the auxiliary switch and clamp diode. However, as will be made clear later, the auxiliary circuit current peak of this topology is reduced, and the timing of the auxiliary switch is also much easier.

The operation of this converter is similar to its PWM counterpart's. The only difference is in the switch turn-on and turn-off transients, during which the auxiliary circuit is actuated to provide soft switching conditions for the main switch S. The simulated waveforms during one switching period are shown in Fig. 2(b). During one switching period, the circuit goes through nine different stages which are listed as (a) through (i) below and which correspond to the subtopologies in Fig. 3. The circuit parasitics, such as semiconductor junction capacitance, and stray inductance, are included in the simulation but ignored in the following description. The operation description starts with switch turn-on transition. Before the main switch turn-on, the inductor current I is conducted by the main diode, the auxiliary current ix is zero, and vx is a constant positive value. In the whole commutation process, the output voltage Vo and inductor current I are assumed to be constant, due to the large capacitance and inductance involved.

(a) Turn-On Transition I [t0, t2] At t0, Sx is turned on, starting the turn-on transition. The auxiliary resonant tank, consisting of Lx and Cx, starts to resonate. The auxiliary current ix resonates from zero to peak, and then decreases towards zero. When ix reaches zero at t1, since the resonant capacitor voltage vx is negative at t1, the auxiliary

circuit continues resonating, and ix reverses its direction and is conducted by Dx, the parallel diode of Sx. Then Sx can be turned off under zero-current and zero-voltage condition, with much reduced power loss. As ix increases in positive value, the current of the main diode is diverted into the auxiliary circuit.

(b) Turn-On Transition II [t2, t3] When ix reaches its positive peak at t2, the current in the main diode is reduced to zero. Then S is turned on under zero-current condition at t2. The turn-on loss is reduced significantly, since the diode reverse recovery is basically eliminated and the current rise rate of the switch after turn-on is limited by the resonant inductor. After t2, ix decreases rapidly towards zero, since now the output voltage Vo is included in the resonant path.

(c) Turn-On Transition III [t3, t4] At t3, ix returns to zero, and Dx is turned off naturally. Since the resonant capacitor voltage vx is positive at t3, the auxiliary circuit continues resonating, and the negative ix is conducted by the clamp diode Dc.

(d) Switch-On Stage [t4, t5] When ix returns to zero again at t4, Dc is turned off naturally. The auxiliary circuit stops resonating, and is disconnected from the main circuit

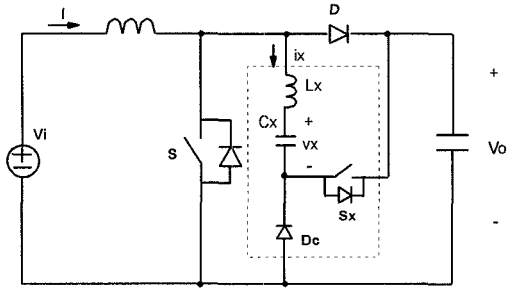

(a) Topology.

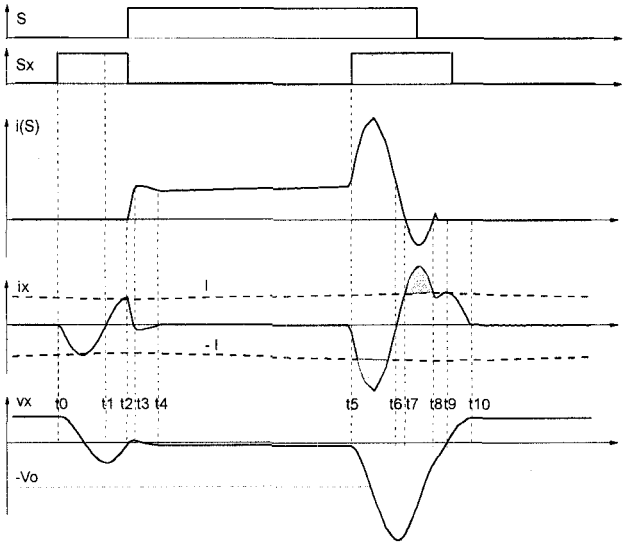

(b) Operational Waveforms.

Fig. 2. An Improved ZCT PWM Converter

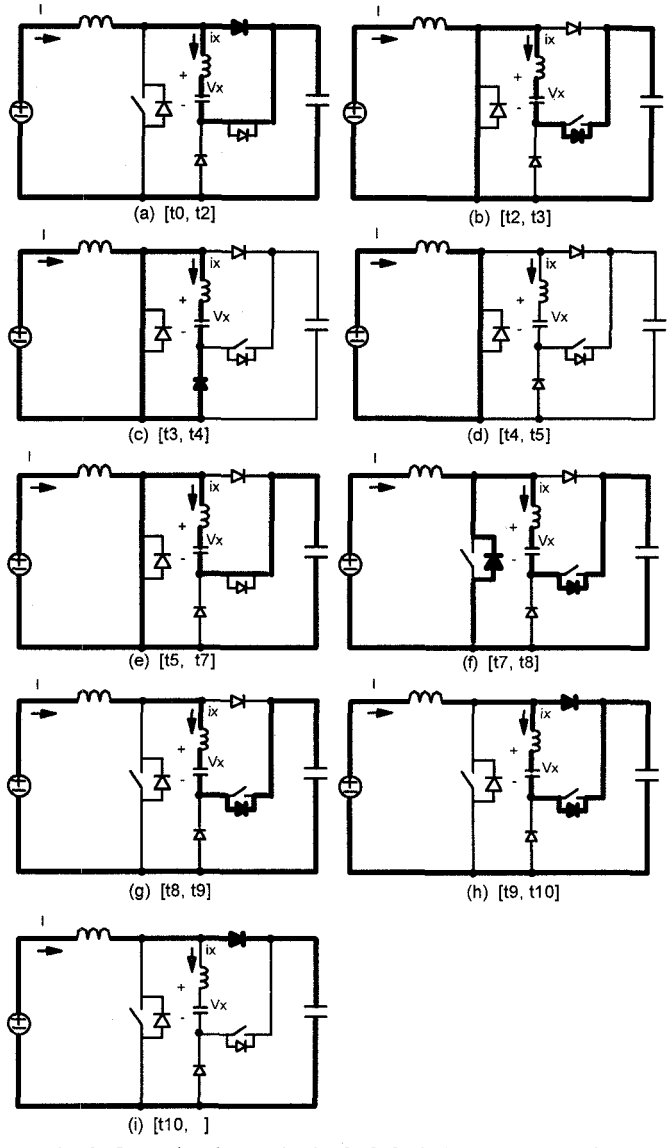

Fig. 3 Operating Stages in the Soft-Switching Commutation.

functionally. The converter resumes its PWM operation. The duration of this stage is determined by the PWM control.

(e) Turn-Off Transition I [t5, t7] Before the main switch is turned off, Sx is turned on at t5. The resonant tank starts to resonate again. The resonant path includes Lx, Cx and output voltage Vo. Current ix is negative and its magnitude increases from zero to peak, and then decreases. When ix returns to zero at t6, Sx is turned off under zero-current condition. Since the resonant capacitor voltage vx is less than -Vo, the auxiliary circuit continues resonating after t6, and the positive ix is conducted by Dx, and the current of the main switch is diverted out into the auxiliary circuit. Since Dx clamps the voltage of Sx at practically zero, the turn-off loss of Sx is largely eliminated.

(f) Turn-Off Transition II [t7, t8] At t7, ix reaches I, and the main switch current is reduced to zero, so S is turned

off under zero-current condition. As ix keeps increasing after t7, the surplus current will flow through the parallel diode of S, and clamp the voltage across S at zero. The gate signal of S can be removed, without causing much turn-off loss.

(g) Turn-Off Transition III [t8, t9] At t8, ix falls to I, and the parallel diode of S stops conducting. Since the main diode is still reversely biased, the main inductor current can only flow through the resonant tank, charging the resonant capacitor linearly.

(h) Turn-Off Transition IV [t9, t10] At t9, vx is discharged to zero and the main diode starts to conduct. The resonant tank begins to resonate again. As ix resonates towards zero, the current in the main diode increases gradually.

(i) Diode On Stage [t10,) When ix returns to zero at t10, the auxiliary circuit stops resonating, and is disconnected from the main circuit functionally. The inductor current is conducted by the main diode, and the converter resumes its PWM operation. The duration of this stage is determined by the PWM control.

Ideally, the peak of ix during the turn-on transition at t2 is the same as the input current I at t9 if the resonant circuit has no power loss. The power loss in the resonant path will reduce the attainable resonant current peak at t2. However, I is smaller at t2 than at t9, considering the current ripple due to finite boost inductance. Therefore, the zero-current turn-on of S is still achievable in a practical circuit.

State-Plane Analysis of the ZCT operation

The difference among the three ZCT schemes can be more easily illustrated by the state plane trajectories. Assuming ideal components, the state plane trajectories of the resonant tank are shown in Fig. 4. The time instants (t0, t1, t2, ...) in Figs. 4(a), 4(b) and 4(c) correspond to the time instants shown in Figs. 1(b), 1(c) and 2(b) respectively. The main switch and main diode current is determined by $I - ix$. The current is conducted by the parallel diode of the main switch when $I - ix$ is negative. During the resonance, the state plane trajectory is part of a circle, and the radius of the circle determines the resonant tank energy and associated conduction loss in the auxiliary circuit. Fig. 4(a) shows the previous ZCT operation of Fig. 1. Obviously, the reverse recovery of the main diode and the turn-on of the main switch are not affected by the ZCT circuit, and could produce high power loss in a practical circuit. The turn-off current of the auxiliary switch is I, which is the same as the turn-off current of the main switch in a hard switched converter. Besides, the timing of the auxiliary switch directly determines the auxiliary circuit current peak, and is critical to the circuit operation. The state-plane trajectories of the ZCT topology with modified control are shown in Fig. 4(b). All devices are now turned on and off with zero-current, but the resonant circle is much larger. Besides, the timing of the auxiliary switch is still critical. The operation of the improved ZCT circuit,

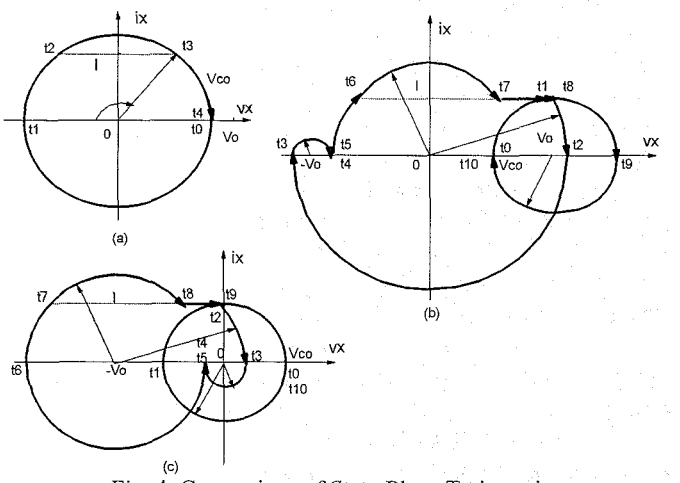

Fig. 4 Comparison of State-Plane Trajectories

shown in Fig. 4(c), has a smaller resonant circle, so less resonant tank energy and less power loss are required. In addition, the auxiliary switch can always be turned off after being turned on for half resonant cycle, so its timing is independent of circuit operation. The control timing during the soft-switching transition then does not need to be changed with operating point variation. This property significantly simplifies the control design.

One distinctive advantage of these ZCT topologies is that all switch devices are switched under zero-current condition. Therefore, switching losses are reduced significantly, so a better utilization of switches can be achieved at a high switching frequency. In addition, snubber circuits are not required to reduce the electrical stress of power devices, and gate drive circuits can be simplified, especially for GTOs. The auxiliary switch has almost no switching loss and switching stress since is turned on and off always with zero-current condition. Low conduction voltage devices, such as GTOs, MCTs and IGBTs, can be used in the auxiliary circuit to reduce its conduction loss. All these factors can be translated into cost savings in a practical application.

III. APPLICATIONS OF IMPROVED ZCT SCHEMES

It is well known that any PWM converter can be viewed as special connections of the PWM cells, each consisting of a switch and a diode connected in a totem pole fashion, such as S and D in Figs. 1(a) and 2(a). The ZCT topologies in Figs. 2(a) and 5(a) can be used as ZCT PWM cells, and easily extended to other PWM converters with the PWM cell concept. Several examples of dc-dc converters with the ZCT scheme in Fig. 2(a) are shown in Fig. 5.

The proposed ZCT topologies are equally applicable to bridge type converters. In a bridge topology, the auxiliary circuits for a top switch and the bottom switch in the same leg can be combined and simplified. Fig. 6(a) shows an example of three-phase ZCT PWM voltage source inverters. The

three-phase ZCT inverter in Fig. 6(a) is topologically similar to modified McMurry inverters for SCRs. However, the operation is different because the auxiliary switches are controlled to improve both turn-on and turn-off performances of the switches.

The voltage stress of the resonant capacitor Cx is about twice that of the switches in the topologies of Fig. 2(a), Fig. 5, and Fig. 6(a). This voltage peak can be reduced by the topology shown in Fig. 6(b). Two series connected auxiliary switches are used for each leg, which is similar to the auxiliary resonant commutated pole (ARCP) converter in [4] with clamp diodes in the auxiliary circuit to reduce the voltage ringing of the auxiliary switches. The low power diodes Dc1 through Dc6 are used to clamp the auxiliary switch voltage. The ZCT circuit is controlled to solve both turn-on and turn-off problems of the switches, which is not achieved in ARCP. Furthermore, the charge balance of the dc-link midpoint is automatically achieved in the ZCT topology. The corresponding state-plane trajectory of the ZCT operation is shown in Fig. 6(c), which is the same as Fig. 4(c) except that vx is shifted by Vo/2 to the right. Therefore, the voltage stress of Cx is now reduced to about 1.5.

Compared to the ZCS scheme in [5], the ZCT topologies in Fig. 6 should have better performance, since they do not have additional components in the main power path, and the voltage stress of all switches is kept at minimum under any operating conditions. Since both turn-on and turn-off problems are solved and the control timing of soft-switching can be fixed for any phase current, the proposed ZCT topologies are very suitable for high power applications.

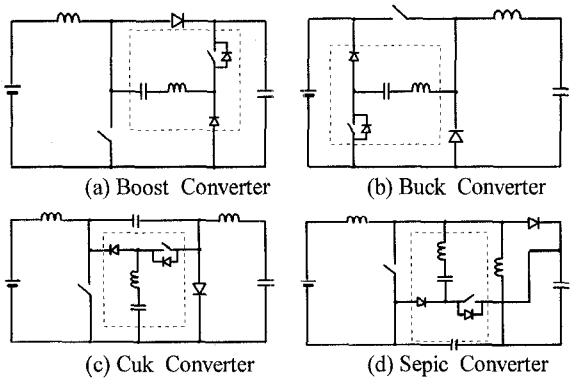

Fig. 5. Examples of ZCT dc-dc converters

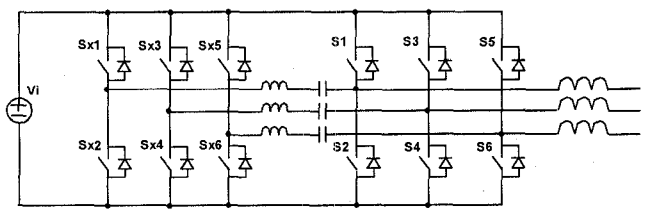

(a) ZCT three-phase inverter.

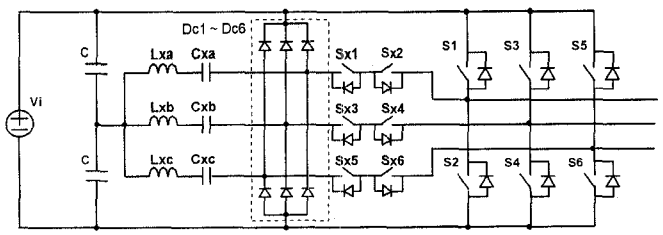

(b) Modified ZCT three-phase inverter.

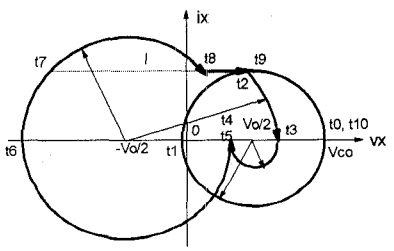

(c) State-trajectory of ZCT in (b).

Fig. 6 Three-phase ZCT Inverters.

IV. DESIGN OF THE ZCT CIRCUIT

It is desired that soft switching can be achieved for all operating conditions. The auxiliary circuit should be designed to achieve zero-current switching with maximum main current while the power loss in the auxiliary circuit is minimized. We will discuss the design issues with the ZCT cell of Fig. 2(a) as an example. Since the turn-off transition is more critical than the turn-on transition, the following design procedure is mainly based on the turn-off requirement. The effect of power loss during the soft-switching commutation and circuit parasitics on circuit operation waveform is not significant, and is ignored in the following analysis for the purpose of simplicity. To effectively reduce switch turn-off loss, the duration of Turn-off Transition II, $T_{off} = T_8 - T_7$, should be long enough for most storage charge of the main switch to recombine. In the following analysis, the design is based on maximum main inductor current, denoted as I. From the state-plane trajectory of Fig. 4(c), we can get:

$$T_{off} = 2\cos^{-1}(m)\sqrt{L_x C_x} = T_0 \cos^{-1}(m)/\pi, \qquad (1)$$

where $m = I / I_{pk}$, $T_o = 2\pi\sqrt{L_x C_x}$. I_{pk} is the resonant peak of ix during turn-off. Assuming vx is zero at t5 without losing much accuracy, we can estimate I_{pk} to be:

$$I_{pk} \approx V_o / Z_0, \qquad (2)$$

where $Z_o = \sqrt{L_x / C_x}$ is the characteristic impedance of the resonant tank.

The choice of T_{off} is device-dependent. Generally, T_{off} should be much longer than the current fall-time of the main switch. A longer T_{off} can be achieved by either increasing I_{pk} or increasing T_0. The design objective is to minimize the conduction loss caused by the soft-switching action for a

given T_{off}. The design optimization requires power loss models for all switches, diodes and reactive components, and is very complex. To simplify the analysis, we assume that the power loss caused by the soft-switching is proportion to the auxiliary current, i.e. the power loss can be represented as a voltage source, whose value is determined by the components in the resonant paths. It is also assumed, without losing much accuracy, that the switch and diodes Sx, Dx, and Dc in the auxiliary circuit have the same conduction voltage drop, while the switch and diodes in the main circuit have the same conduction voltage drop. Since the auxiliary current is always conducted by Lx, Cx, a switch or a diode in the auxiliary circuit, the equivalent voltage drop for the power loss in the auxiliary circuit , denoted as V_c in the following discussions, is constant for all operation stages in the commutation. Howvever, the conduction loss of the main power stage is reduced for ix>0, but increased for ix<0. The voltage drop of the main switch (or diode) is assumed to be $1/k$ of the total voltage drop in the auxiliary circuit, i.e. V_c/k. From Fig. 4(c), we can see that the state-plane trajectory of soft-switching action can be approximated as two circles: one with a radius of V_o, the other with a radius of $Z_0 I$. Since the charge exchange of the resonant capacitor equals to the integral of the auxiliary current, the energy loss in the auxiliary circuit per switching cycle can be calculated as:

$$E_1 = V_c * C_x(4V_o + 4Z_0 I) = 2(1+m)V_c I_{pk} T_0 / \pi \quad (3)$$

The current in the main switch or the main diode is $I - ix$. Since ix changes form negative to positive in the resonance, its net effect on the main circuit conduction loss is nullified for the portion $|ix| \le I$. So the addtional conduction loss in the main circuit caused by the soft switching is determined only by the portion of ix where ix is higher than I in magnitude, as shown in the shaded area in Fig. 2(b). The resultant energy loss per switching cycle can be calculated as:

$$E2 = 2(\sqrt{1-m^2} - 2m\cos^{-1}(m))/k]V_c I_{pk} T_o / \pi . \quad (4)$$

Combining (3) and (4), we get the total conduction loss caused by the soft-switching commutation:

$$\Delta E = E_1 + E_2 = 2V_c I_{pk} T_o * [(1+m) + (\sqrt{1-(m)^2} - m\cos^{-1}(m))/k]/\pi, \quad (5)$$

In a specific application, V_c, T_{off} and maximum input current I are given. Therefore, the design objective is to minimize the normalized energy loss:

$$E_n = \Delta E / (2V_c I T_{off}) = \frac{[(1+m) + (\sqrt{1-m^2} - m\cos^{-1}(m))/k}{m\cos^{-1}(m)}, \quad (6)$$

(6) is plotted in Fig. 7(a) as a function of m for different values of k. In a practical converter, k is usually within the range of *2~4*. A good design should select Lx and Cx so that E_n is around its minimum for maximum main inductor current. It can be seen from Fig. 7(a) that a good design should have m in the range of *[0.5, 0.7]*.

Once $m = M$ is chosen, Lx and Cx can be calculated from (1) and (2):

$$L_x = \frac{V_o T_{off}}{2MI\cos^{-1}(M)}, \quad C_x = \frac{MT_{off} I}{2V_o \cos^{-1}(M)} \quad (7)$$

E_n for different inductor current i can be written as a function of normalized inductor current $I_n = i/I$:

$$E_n = \frac{[(1+MI_n) + (\sqrt{1-(MI_n)^2} - MI_n \cos^{-1}(MI_n))/k}{M\cos^{-1}(M)}, \quad (8)$$

(8) is plotted out in Fig. 7(b) for $k = 2$ and several possible values of M. From Fig. 7(b), it can also be seen that although an optimum design, here $M = 0.6$, might have lowest energy loss in the whole current range, En is not very sensitive to M, so M can be chosen in a relatively large range around its optimum value without significantly reducing circuit efficiency. Fig. 7(b) can also be used to evaluate the circuit efficiency at different currents.

The above equations are based on simplified power loss models of the components. A pratical converter will have much more complex loss models for its components, and the optimum design can only be achieved through experiment or detailed simulation. Fig. 7 can give some design insight, and serve as a starting point for the optimization. In a practical design, the main concern is the maximum power loss instead of the efficiency over the entire operation range. The proposed ZCT schemes can be used to reduce the worst case power dissipation (i.e. at the maximum load) in the power devices. It should be noted that I_{pk} is almost constant even if the input current is reduced at light load. From Fig. 7(b), we can see that the additional conduction energy loss caused by soft switching does not change much even if the main current is reduced from its maximum to zero. Therefore, the ZCT operation should be disabled at light load to achieve good efficiency. Fortunately, the thermal and electrical stresses of devices are lower at light load, and soft-switching function is not really required. Another measure to improve circuit efficiency is to use coupled saturable inductors in the auxiliary circuit, as is shown in Fig. 8. Lm is saturated when I and ix are not equal. However, when ix is about the same as I at t2 and t7, Lm gets out of saturation, and presents a high inductance to the resonant tank. With Lm, the duration of the main switch and diode zero current state is increased, and the conduction loss in the turn-off commutation is reduced. With Lm included in the circuit, T_o (calculated with Lm saturated) can be reduced by about 30% for the same T_{off}, which results in considerably lower power loss.

From Fig. 4(c), we can see that the conduction duration of the auxiliary switch is always 50% of the resonant cycle, i.e. $T_0/2$. The main switch can be turned on or off around

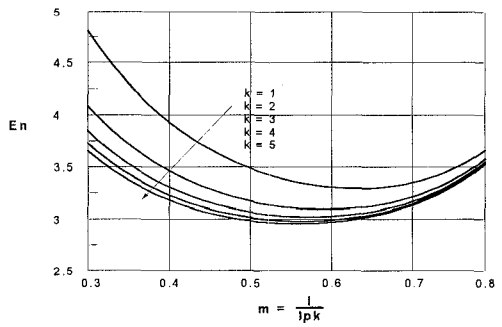

(a).

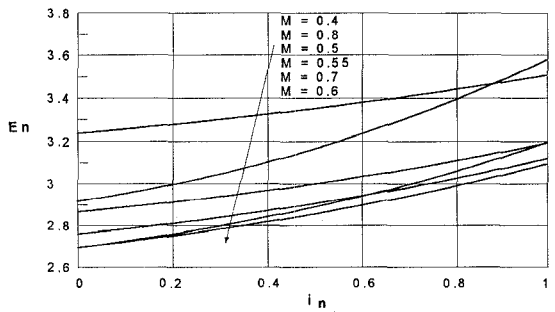

(b).

Fig. 7. Design curves for commutation circuit

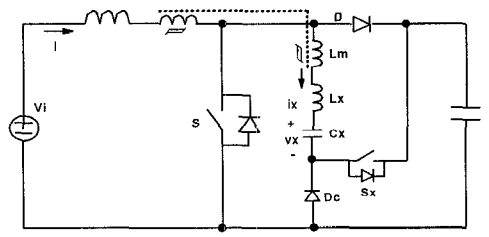

(a). Topology

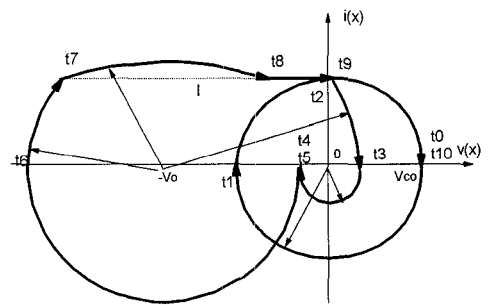

(b). State-plane trajectory

Fig. 8. ZCT converter with coupled inductor

the second resonant peak of ix, so the delay between the auxiliary switch turn-on signal and the main switch turn-on or off signals can be set to about $3T_0 / 2$. Therefore, the control timing of the soft switching is completely independent of circuit operating point, which greatly simplifies the control design.

V. EXPERIMENTAL RESULTS

Two prototype half-bridge converters with the ZCT cells in Fig. 2(a) and Fig. 6(b) are built and tested. The experimental circuits are shown in Figs. 9(a) and 9(b). The switching frequency is 20 kHz in both circuits. Since an MCT device has the typical switching characteristics of high power devices, the commercially available MCT switch MCTV75P60E1 is used for the main switches, and the auxiliary switches are implemented as IGBTs IRGBC30U, which has much lower current capability than the MCT main switch. Fig. 10 shows the experimental waveforms. It can be seen that the circuit waveforms comply with the theoretical analysis and simulation. In Fig. 10(a), a small RC snubber is used to damp the ringing of Va when both auxiliary switches are off. Fig. 11 shows the measured efficiency, which would be the full-load efficiency for a practical application under different voltages, but with the same *M*. In the experiment, the hard switched converter can only operate up to 300 V input voltage, due to the limited safe operating area. However, the soft-switched converters can operate up to 430 V. This shows that the soft-switching schemes reduce the switch stress and improve device utilization. In addition, considerable efficiency improvement is achieved in both ZCT schemes. The topology in Fig. 9(a) has higher efficiency than the topology in Fig. 9(b) due to the reduced conduction loss in the auxiliary circuit. However, the auxiliary switches in Fig. 9(b) have less voltage ringing, and the resonant capacitor voltage rating is also lower. Therefore, the topology shown in Fig. 9(b) could be more advantageous in some high voltage applications. Because the switching loss in hard switched converters increases greatly at higher switch junction temperature, the efficiency improvement of the soft switching schemes will be higher in a practical application.

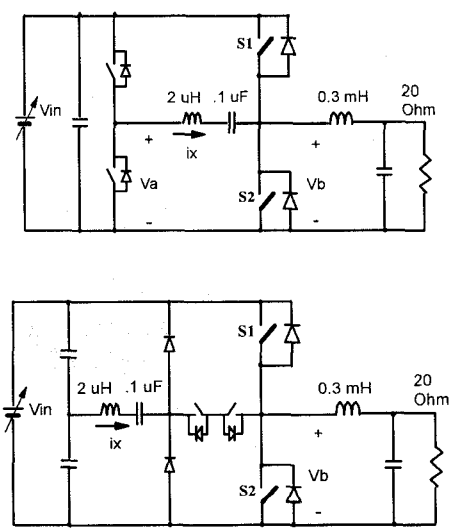

Fig. 9. Experimental circuits

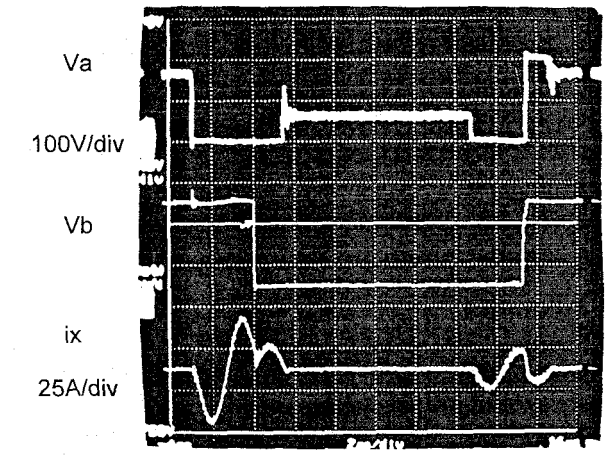

ZCT scheme in Fig. 10(a)

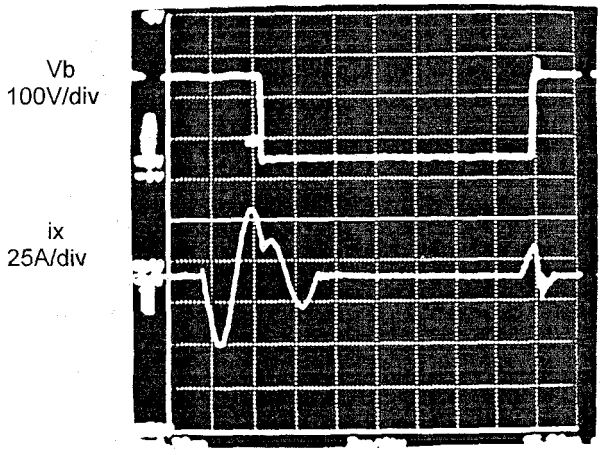

ZCT scheme in Fig. 10(b)

Fig. 11. Experimental Waveforms

VI. CONCLUSIONS

Novel ZCT topologies are proposed for high power applications. With the help of a low power auxiliary ZCT circuit, the main switches are turned off under zero-current condition, practically eliminating all turn-off losses. The turn-on current of the main switches is also reduced to around zero, so switch turn-on loss and diode reverse recovery are also significantly reduced. The auxiliary switches are also turned on and off with zero current, and can be implemented with low saturation voltage devices. The switches in the proposed ZCT converter have much lower switching loss and switching stress than in a conventional converter, and therefore can operate at a much higher switching frequency and achieve much higher power density due to smaller reactive components. Also, the snubbers can be reduced or eliminated in the ZCT converter, and drivers for GTOs can be simplified. As a result, the implementation of the ZCT converter is simpler than with a conventional topology, and its cost may be reduced while its efficiency, EMI emissions, reliability, and dynamic performance are improved. The proposed topologies are relatively simple to design, and can be used in various dc-dc and three-phase converters. Experimental results prove that significant efficiency improvement can be achieved with the ZCT circuit.

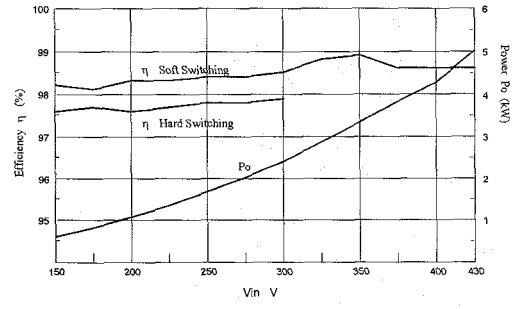

(a) Prototype of Fig. 10(a)

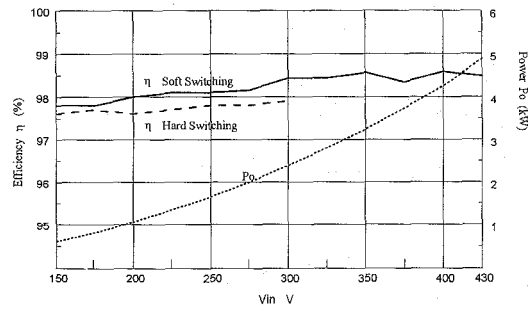

(b). Prototype of Fig. 10(b)

Fig. 12 Measured efficiency

References

[1] G. Hua, E. Yang, Y. Jiang, and F. C. Lee, "Novel zero-current transition PWM converters," in *IEEE-PESC*, 1993, pp.538-544.

[2] G. K. Dubey, "Classification of commutation methods," in *IEEE-IAS Annu. meet.*, 1981, pp. 895 - 909.

[3] W. McMurray, "Thyristor commutation in dc choppers-a comparative study," *IEEE Trans. Ind. Applcat., vol. 14*, pp. 547-558, 1978.

[4] R. W. De Doncker and J. P. Lyons, "The auxiliary resonant commutated pole converters", in *IEEE-IAS Annu. meet.*, 1990, pp.1228-1235.

[5] P. Tomasin, "A novel topology of zero-current switching voltage-source PWM inverter for high power applications," in *IEEE-PESC*, 1995, pp. 1245-1251.

[6] D. M. Divan, "Resonant dc link converter- a new concept in power conversion", in *IEEE-IAS Annu. meet.*, 1986, pp. 648 - 656